TEMPERATURE DISTRIBUTION IN THE WALL OF A CHANNEL BETWEEN FINS CONTAINING A BOILING LIQUID

V. K. Shcherbakov and L. V. Kovalenko

UDC 536.242:536.423.1

Measurements on the temperature distribution in a fin with water boiling in the channel between fins are reported. The results are compared with the analytical solution for the one-dimensional case.

There are several studies [1-4] on the temperature patterns in finned heat exchangers with liquid boiling in the channels between fins; however, these are restricted to the temperature patterns in the fins when boiling occurs in a large volume of liquid initially at the boiling point. A numerical solution has been given [5] for the temperature pattern when a liquid below the boiling point is forced through fin channels and boils there.

A study has been made of the temperature distribution in a cylindrical copper wall of d_{in} = 14 mm having straight longitudinal fins ($2\delta_f$ = 1.7 mm, 2b = 4 mm, h = 4 mm, δ_w = 2 mm in Fig. 2) with radial heat supply to the internal smooth surface and with boiling in the channels between the fins, where water below the boiling point is injected.

The system was built as a closed-loop circulation system made of stainless steel, and this could operate with chemically desalinated water at p = 2-5 bar, w = 0.5-5 m/sec, Δt_{un} = 40-90°C, and heat inputs of $q_1 = (0.1\text{-}5) \cdot 10^6$ W/m^2.

The working section (Fig. 1) consisted of an outer jacket and coaxial component 3 with current-carrying rods soldered to the top 1 and bottom 5. The gaps between the component and the rods had similar external fins and were fitted with the copper inserts 2 in order to provide channels uniform along the length l. This also ensured hydrodynamic stabilization over the working section, since l/d_{eq} = 50. Part of the outer jacket was made of polished lucite 4, which provided for visual observation of the state of the cooling surface between the fins.

Uniform heat loading was provided at the inner surface at values up to q_1 = 5 MW/m^2 by virtue of the special design (Fig. 2). The system consisted of the heater 1, which was a thin-walled stainless-steel tube (Ø14 × 0.6) heated by direct current and covered by a layer of high-temperature insulation 2 of thickness 20-30 μm, working with a cylindrical finned wall 3 (Ø18 × 2), in which straight longitudinal fins had been milled. The coated heater 1 was inserted within the finned cylindrical component 3 after the latter had been heated to about 500°C. This mode of assembly provided high pressure at the contact surface when tube 1 was heated electrically and the wall 3 was cooled by water; consequently, there was little thermal resistance to the radial heat flow.

The temperature of the finned wall was measured with copper–Constantan thermocouples mounted in holes (Ø 0.3 mm) which were drilled to a depth of 15 mm from the end of the finned wall (Fig. 2). The thermocouples were placed at the point of greatest hazard (the exit point for the water) within the cross section of the system (Fig. 1), the position being such that end leakage of the heat had virtually no effect on the temperature pattern. The appropriate section was determined by electrical simulation of the two-dimensional case with an R-network model. Distortion of the temperature pattern by the thermocouples was minimized by placing the latter in adiabatic symmetry planes in the fins and in the wall between the fins at various heights. The thermocouples were perpendicular to the plane of temperature measurement (Fig. 2). Not more than one thermocouple was placed in each fin and in each part of the wall between the fins.

The general temperature apttern in the finned wall was determined by solving the heat-conduction problem [6]; the two-dimensional inverse problem was solved by electrical simulation with an R-network integrator [7].

Kiev Polytechnic Institute. Translated from Inzhenerno-Fizicheskii Zhurnal, Vol. 35, No. 3, pp. 404-409, September, 1978. Original article submitted September 19, 1977.

 0022-0841/78/3503-1022$07.50

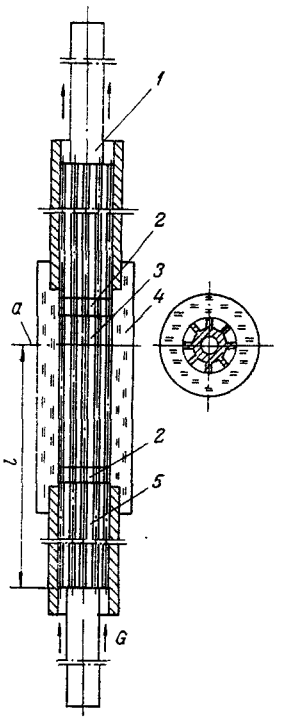

Fig. 1. Working component (*a* is the working section).

The temperatures $t_1 - t_{10}$ were measured on the symmetry lines of the fins and walls (Fig. 2), and the values were transferred to the corresponding points in the sector, which was defined by the geometrical and thermal symmetries of the fin system (Fig. 3). The measured temperatures, as well as the measured input heat fluxes, the cooling-water temperature, and the thermophysical parameters of the material, were used together with values from the analog simulation in solving the inverse problem; this made it possible to determine the temperature pattern in the section and the distribution of the heat-transfer coefficient over the cooled perimeter.

The errors arising in solving the inverse condition problem were $\delta(t)$ for the temperature of the space between fins and $\delta(\alpha)$ for the heat-transfer coefficient on the cooling surface; these values were calculated in accordance with the recommendations of [10, 11] on the basis of the error of measurement for the temperatures $t_1 - t_{10}$ and the input q_1, the results being $\delta(t) \leq 8\%$ and $\delta(\alpha) \leq 16\%$.

The methods of measurement and solution were checked out by comparing the mean values $\bar{\alpha}_c$ for the heat-transfer coefficient in the channel between fins derived from the electrical model via the measured data for convective heat transfer and the values calculated from the following equation [8]:

$$\bar{\alpha}_c = 0.021 \frac{\lambda_L}{d_{eq}} \mathrm{Re}_{L,d_{eq}}^{0.8} Pr_L^{0.43} \left(\frac{Pr_L}{Pr_W}\right)^{0.25} \varepsilon_l, \quad (1)$$

which applies for turbulent flow, as occurred in the experiments.

The values for $\bar{\alpha}_c$ obtained in preliminary trials (about 80 values) covered the range $\mathrm{Re} = (8\text{-}40) \cdot 10^3$ and lay around the line derived from (1) with a maximum spread of ±12%, which is no greater than the error of the formula and which allows one to use this method to examine the temperature pattern in such a finned wall with bubble boiling in the channels between the fins when the water is initially below the boiling point.

Figure 3 shows the temperature pattern in such a wall and the pattern of the heat-flux density around the perimeter for these cooling and heating conditions; Fig. 3 shows that the temperature at the cooled surface varies only slightly between the fins, but there is considerable heat leakage to the fins when the conductivity of the material is high, $\lambda_m = 380$ W/m$^2 \cdot$°C. Since the ratio of the maximum heat-flux density q_2^{max} in the x = b section to the heat load q_1 is $\varphi_b = (q_2^{max} \cdot R_2)/(q_1 \cdot R_1) = 0.72$, the heat leak in the wall from the symmetry plane of the channel is 28%; therefore, this fin symmetry is reasonably effective under these conditions, since it reduces q_2^{max} by 28%.

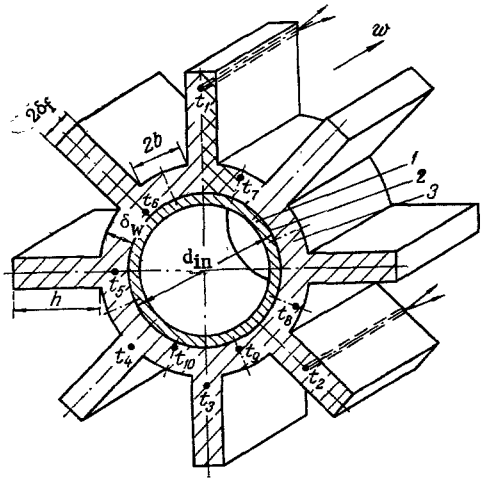

Fig. 2

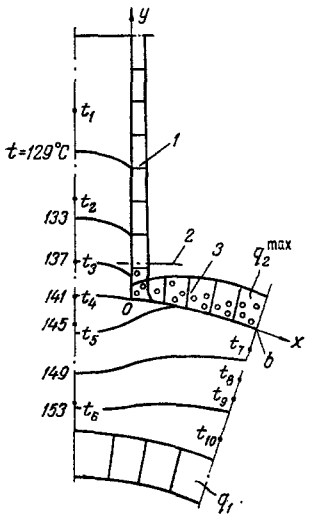

Fig. 3

Fig. 2. Temperature measurement in the working section of a finned wall.

Fig. 3. Temperature pattern in a sector of a finned wall for q_1 = 1.87 MW/m^2, w = 1.3 m/sec, Δt_{un} = 38.4°C, and p = 2.5 bar: 1) region of convective heat transfer; 2) boundary of boiling; 3) region of bubble boiling.

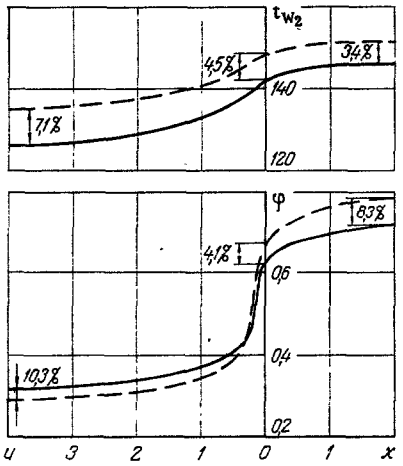

Fig. 4. Distribution around the perimeter of a channel between fins of the wall temperature t_{w_2}, (°C) and dimensionless heat-flux density φ; x and y are in mm.

We processed the measurements in the solution of the inverse problem for all the runs involving bubble boiling; this showed that the fins reduced q_2^{max} in particular cases by up to 45% under these conditions.

Also, the data were processed to define the temperature pattern around the perimeter of the channel, which was compared with the analytical solution [9]. The solution in [9] was derived by joint one-dimensional solution of the heat-conduction problem for a planar wall and also for a straight longitudinal fin; a BÉSM-4M computer was used.

The inverse solution derived from the measurements was compared with the calculation of [9] for a finned wall (Fig. 3) as shown in Fig. 4; this figure shows the temperature distribution around the perimeter of the wall

t_{w_2} and the dimensionless heat-flux density $\varphi = (q_2 \cdot R_2)/(q_1 \cdot R_1)$; the abscissa is the current coordinate on the fin and wall, while the ordinate passes through the point where the fin and the wall between the fins meet. The solid lines are measured values of t_{w2} and φ, while the dashed lines are those computed in [9].

Figure 4 shows that there is satisfactory agreement for t_{w_2} and φ in both cases; the calculated t_{w_2} and φ exceed the observed values by not more than 3.4% for t_b or 4.5% for t_0, which corresponds to the points of most importance for design purposes, namely, x = b and x = 0 on the perimeter (Fig. 3); the discrepancy for φ_b was 8.3%.

The inverse solution via the experiments was compared with the analytical solution by computer [9] for the corresponding boundary conditions for all the runs; it was found that the system of equations of [9] defines the temperature pattern and the heat-flux distribution around the perimeter with good reliability under these conditions. The temperatures and heat fluxes at x = b and x = 0 calculated from the equations of [9] exceed those found by solving the inverse problem by up to 5% for t_b, up to 7.5% for t_0, and up to 10% for φ_b.

These results therefore show that a finned wall made of material of high conductivity working with a liquid boiling in the gaps while in forced motion can reduce the heat-flux density substantially by comparison with smooth walls, and this can substantially increase the power handled.

NOTATION

q is the heat flux density;
φ is the dimensionless density of outgoing heat flux;
α, λ are the heat-transfer coefficient and coefficient of thermal conductivity;
t is the temperature;
ϑ is the excess temperature;
Δt_{un} are the deviation from saturation temperature t_{sat};
p, w are the pressure and velocity of liquid;
δ_f, h are the half-thickness and height of fin;
b, δ_w are the channel half-width and wall thickness;
R is the radius;
d is the diameter;
l is the channel length;
Re, Pr are the Reynolds and Prandtl numbers.

Indices

L is the liquid
m is the material;
w is the wall;
f is the fin;
o is the fin base;
i is the point of onset of boiling;
c is the convection;
bo is the boiling;
1 is the heating surface;
2 is the cooling surface;
max is the maximum value;
eq is the equivalent.

LITERATURE CITED

1. L. I. Roizen and G. R. Rubin, Inzh.-Fiz. Zh., 22, No. 1 (1972).
2. S. A. Kovalev and L. F. Smirnova, Teplofiz. Vys. Temp., 6, No. 4 (1968).
3. Shih Chien-cheng and J. W. Westwater, in: Heat Transfer: Proceedings of the Fifth International Conference, Tokyo, Vol. 4 (1974).
4. M. S. Lai and J. J. Hsu, AIChE, J., 4, No. 4 (1967).
5. M. Cumo, S. Lopez, and G. C. Pinchera, Eng. Progr. Symp., 61, No. 59 (1965).
6. A. G. Temkin, Inverse Methods in Heat Conduction [in Russian], Énergiya, Moscow (1973).
7. E. A. Krasnoshchekov, V. S. Protopopov, and A. T. Igamberdiev, Teplofiz. Vys. Temp., 7, No. 6 (1969).

8. M. A. Mikheev and I. M. Mikheeva, Principles of Heat Transfer [in Russian], Énergiya, Moscow (1973).
9. V. K. Shcherbakov and L. V. Kovalenko, Inzh.-Fiz. Zh., 31, No. 1 (1976).
10. L. A. Kozlova, Solution of Nonlinear Heat-Conduction Problems [in Russian], Naukova Dumka, Kiev (1976).
11. R. S. Guter and B. V. Ovchinskii, Principles of Numerical Analysis and Mathematical Processing of Experimental Data [in Russian], Nauka, Moscow (1970).

EXPERIMENTAL STUDY OF LAMINAR-TO-TURBULENT FLOW TRANSITION UNDER THE ACTION OF ACOUSTIC OSCILLATIONS

A. N. Shel'pyakov and G. P. Isupov

UDC 532.517

Experimental data are given on the effects of acoustic oscillations at frequencies up to 100 kHz on free laminar flow.

Acoustic agitation of a free laminar jet promotes the transition to turbulent flow for small Reynolds numbers Re [1]. When the acoustic source is removed, the jet returns to the laminar state.

The results of experimental investigations of the effect of acoustic oscillations on a free jet at a maximum frequency of 10 kHz are given in [1].

Here we discuss the results of experiments on the effect of acoustic oscillations on a free jet at frequencies up to 100 kHz.

The experiments were conducted with nozzle–nozzle jet elements having capillary diameters of 0.4 to 0.9 mm.

A typical curve of the pressure variation in the receptor duct as a function of the pressure in the injector duct is given in Fig. 1 (curve 2). The three main flow regimes (laminar, transition, and turbulent) correspond to the three intervals $0a$, ab, and bc of curve 2 in Fig. 1.

Theoretical and experimental studies of the laminar-to-turbulent transition [2] have shown that at the initial instant one or more small-amplitude oscillations arise in the flow in a single phase (Tollmien waves), subsequently evolving into more complex three-dimensional modes (Benney–Lin waves). These waves are broken up by vigorously growing small-scale pulsations (zone of secondary instability), which emerge as Emmons spots, continue to develop downstream, and induce turbulence throughout the entire flow.

A definite analogy exists between the development of acoustic emission from a jet and the transition of the latter from laminar to turbulent flow.

A pure laminar jet (lower half of interval $0a$) does not emit sound. As the injection pressure is increased (toward the end of interval $0a$) the jet begins to emit sound with a distinct single frequency (in our situation 5.3 kHz). A further increase in the injection pressure (interval ab) causes an increase in the total noise level of the jet, and the 5.3-kHz discrete component vanishes. We measured the acoustic characteristics of the jet with a microphone and analyzed them on the screen of an S1-19B oscilloscope.

The action of acoustic waves emitted by a jet on the flow regime of the latter is confirmed by the experiment described below. The objective of the experimental was to determine the acoustic emission component exerting the greatest influence on the evolution from laminar to turbulent flow.

The experimental arrangement is shown schematically in the inset of Fig. 1. It consists of the capillaries separated by a distance l. One capillary is the injector, and the other the receptor. A reflecting surface in the form of an aluminum plate with an area of 55×25 mm^2, thickness of 1 mm, and microroughness height $R_Z = 3.2$ is set up at a distance L from the common axis of the capillaries. The experimental results are represented by curves 1 and 3 in Fig. 1 and the curve in Fig. 2.

Votkinsk Branch, Izhevsk Mechanics Institute. Translated from Inzhenerno-Fizicheskii Zhurnal, Vol. 35, No. 3, pp. 410-414, September, 1978. Original article submitted July 21, 1977.

 0022-0841/78/3503-1026$07.50